Journal of Biomechanics 42 (2009) 1212–1217

Contents lists available at ScienceDirect

Journal of Biomechanics

journal homepage: www.elsevier.com/locate/jbiomech
www.JBiomech.com

Systematic error in mechanical measures of damage during four-point bending fatigue of cortical bone ☆

Matthew D. Landrigan, Ryan K. Roeder *

Department of Aerospace and Mechanical Engineering, The University of Notre Dame, Notre Dame, IN 46556, USA

ARTICLE INFO

Article history:
Accepted 12 March 2009

Keywords:
Fatigue microdamage
Compact bone
Cortical bone
Elastic modulus
Creep
Four-point bending

ABSTRACT

Accumulation of fatigue microdamage in cortical bone specimens is commonly measured by a modulus or stiffness degradation after normalizing tissue heterogeneity by the initial modulus or stiffness of each specimen measured during a preloading step. In the first experiment, the initial specimen modulus defined using linear elastic beam theory (LEBT) was shown to be nonlinearly dependent on the preload level, which subsequently caused systematic error in the amount and rate of damage accumulation measured by the LEBT modulus degradation. Therefore, the secant modulus is recommended for measurements of the initial specimen modulus during preloading. In the second experiment, different measures of mechanical degradation were directly compared and shown to result in widely varying estimates of damage accumulation during fatigue. After loading to 400,000 cycles, the normalized LEBT modulus decreased by 26% and the creep strain ratio decreased by 58%, but the normalized secant modulus experienced no degradation and histology revealed no significant differences in microcrack density. The LEBT modulus was shown to include the combined effect of both elastic (recovered) and creep (accumulated) strain. Therefore, at minimum, both the secant modulus and creep should be measured throughout a test to most accurately indicate damage accumulation and account for different damage mechanisms. Histology revealed indentation of tissue adjacent to roller supports, with significant sub-surface damage beneath large indentations, accounting for 22% of the creep strain on average. The indentation of roller supports resulted in inflated measures of the LEBT modulus degradation and creep. The results of this study suggest that investigations of fatigue microdamage in cortical bone should avoid the use of four-point bending unless no other option is possible.

1. Introduction

Various methods have been used to measure the accumulation of fatigue microdamage via changes in mechanical properties. The elastic modulus or stiffness degradation is most commonly reported as a ratio or percent loss measured by (1) the maximum beam deflection using linear elastic beam theory (LEBT) (Boyce et al., 1998; Danova et al., 2003; Diab et al., 2006; Diab and Vashishth, 2005), (2) the secant modulus or stiffness (Cotton et al., 2005; Fleck and Eifler, 2003; Gibson et al., 1995; Moreno et al., 2006; Pattin et al., 1996; Schaffler et al., 1989; Schaffler et al., 1990; Winwood et al., 2006a,b; Zioupos et al., 1996), (3) the tangent modulus or stiffness (Akkus et al., 2003; Burr et al., 1998; Gibson et al., 1995; Jepsen and Davy, 1997; Pidaparti et al., 2000), and (4) the unloading modulus or stiffness (Fleck and Eifler, 2003). Other mechanical measures of fatigue damage have included creep or "plastic" strain (Cotton et al., 2003, 2005; Fleck and Eifler, 2003; Moreno et al., 2006; Winwood et al., 2006a,b), cyclic energy dissipation (Pattin et al., 1996) or elastic strain amplitude (Fleck and Eifler, 2003; Winwood et al., 2006a,b), and viscoelastic relaxation or recovery (Jepsen and Davy, 1997; Joo et al., 2007).

The initial modulus or stiffness of a specimen is often measured prior to fatigue testing in order to normalize tissue heterogeneity to a prescribed maximum strain (Boyce et al., 1998; Caler and Carter, 1989; Cotton et al., 2005; Diab et al., 2006; Diab and Vashishth, 2005; Gibson et al., 1995; Pattin et al., 1996; Pidaparti et al., 2000; Sobelman et al., 2004). Cyclic preloading at 100 N for 20 cycles has been commonly adopted for this purpose whether utilizing uniaxial loading with a cross-sectional area of 7–8 mm^2 (Caler and Carter, 1989; Cotton et al., 2005; Pattin et al., 1996) or four-point bending with a 4×4 mm beam cross section (Boyce et al., 1998; Diab et al., 2006; Diab and Vashishth, 2005). Under these conditions the maximum stress of the non-uniform stress distribution in four-point bending is approximately four times greater than the uniform stress of 12–14 MPa produced by uniaxial loading. In four-point bending of machined beams, the

☆ Funding Sources: US Army Medical Research and Materiel Command (W81XWH-06-1-0196) through the Peer Reviewed Medical Research Program (PR054672), National Institutes of Health (AR049598).

* Corresponding author. Tel.: +1 574 631 7003; fax: +1 574 631 2144.
E-mail address: rroeder@nd.edu (R.K. Roeder).

0021-9290/$ - see front matter © 2009 Elsevier Ltd. All rights reserved.
doi:10.1016/j.jbiomech.2009.03.016

specimen modulus during preloading and fatigue is often calculated using LEBT as

$$E = \frac{3PL}{4bh^2\varepsilon} \quad (1)$$

where P is the applied load, L is the outer support span, $L/4$ is the distance between the inner and outer supports, b is the specimen width, h is the specimen height, and ε is the maximum strain based on the beam deflection (Boyce et al., 1998; Diab et al., 2006; Diab and Vashishth, 2005; Gibson et al., 1995; Griffin et al., 1999; Sobelman et al., 2004). The measured initial modulus and a prescribed maximum initial strain are then used to determine a normalized applied load for fatigue testing using Eq. (1).

In an increasing number of studies, specimens are loaded to a specified modulus or stiffness degradation to generate controlled levels of damage (Boyce et al., 1998; Danova et al., 2003; Diab and Vashishth, 2005). However, this practice assumes that measures of modulus or stiffness degradation are free of systematic error. Therefore, the objective of this study was to examine sources of systematic error in mechanical measures of microdamage during cyclic four-point bending fatigue via two experiments. The aim of the first experiment was to establish the effect of the preload level on the initial specimen modulus defined using LEBT and the subsequent modulus degradation during fatigue. The aim of the second experiment was to directly compare different mechanical measures of damage accumulation. The results of these experiments suggested several recommendations for standardization of fatigue testing methods.

2. Methods

2.1. Experiment 1: effects of the preload level

Ten parallelepiped beams, nominally 4 × 4 × 50 mm, were prepared from the mid-diaphysis of bovine tibiae on a computer numerical controlled mini-mill and randomly assigned to two groups. All specimens were wrapped in gauze, hydrated, and stored at −20 °C in airtight containers during interim periods.

The effect of the preload level on the initial specimen modulus defined using LEBT was determined by loading two groups of five specimens in four-point bending fatigue with a minimum load of 4 N and a maximum load that either increased from 40 to 300 N by 20 N every 30 cycles, or decreased from 300 to 40 N by 20 N every 30 cycles. All specimens were preloaded with the periosteal surface in tension under cyclic four-point bending at 2 Hz in de-ionized water at ambient temperature using an electromagnetic test instrument (ELF 3300, Bose Corporation, Eden Prairie, MN). The loading fixture comprised 6.35 mm diameter roller supports with a 40 mm outer span and a pivoting 20 mm inner span. All preloading tests were concluded within a 4 min. total duration, eliminating concerns due to testing in de-ionized water (Gustafson et al., 1996). The initial LEBT modulus was calculated from the maximum load and deflection using Eq. (1) and reported as the mean (±standard deviation) for each preload level. Beam deflections were measured via a linear variable displacement transducer (±0.025 mm sensitivity) at the inner supports and converted to strain using LEBT as

$$\varepsilon = \frac{6h\delta}{L^2} \quad (2)$$

where h is the specimen height, δ is the maximum deflection at the inner supports, and L is the outer support span.

Specimens in both preloading groups were randomly reassigned to two groups of five specimens that were tested in four-point bending fatigue under load control with a minimum load of 4 N and the maximum load normalized to 6000 μstrain using Eq. (1) and the initial LEBT modulus (E_o) determined from a preload of either 100 or 200 N (Fig. 1). All tests were conducted at 2 Hz in phosphate buffered saline at 37 °C and were concluded at 400,000 cycles without failure. The level of strain for normalization was chosen to not exceed the monotonic yield point of the specimens, which was determined to range between 8000 and 11,000 μstrain on specimens originating from the same tissue source.

2.2. Experiment 2: mechanical measures of damage accumulation

Ten additional specimens were prepared from bovine tibiae as described above. All specimens were loaded with the periosteal surface in tension under cyclic four-point bending at 2 Hz in phosphate buffered saline at 37 °C for 400,000 cycles without failure. Specimens were preloaded at 175 N for 20 cycles to measure the initial LEBT modulus, followed by load-controlled fatigue with a minimum load of 4 N and the maximum load normalized to 6000 μstrain. Note that the maximum load ranged 171–208 N (81–100 MPa) for various specimens.

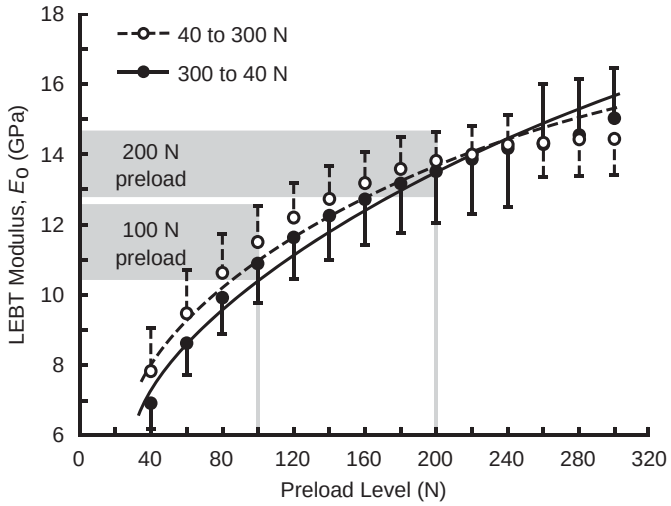

Fig. 1. The dependence of the initial specimen modulus measured using linear elastic beam theory (LEBT) on the magnitude of the applied preload for specimens loaded from 40 to 300 N and 300 to 40 N, increasing or decreasing, respectively, the load by 20 N every 30 cycles. Error bars show one standard deviation. Data was fit by nonlinear least squares regression using a power law ($R^2 = 0.78$ and 0.80, respectively). Shaded regions show the range of initial specimen moduli, E_o, for preload levels of 100 and 200 N employed for the measurements in Fig. 3.

The LEBT modulus, secant stiffness, loading stiffness, unloading stiffness, and creep strain were determined from data collected at 250 points per loading cycle (Fig. 2). The LEBT modulus was calculated from the maximum load and deflection (Fig. 2a) using Eqs. (1) and (2). The secant stiffness was measured as the slope of the line connecting the minimum and maximum load and deflection for a given loading cycle. The loading and unloading stiffness was determined by a linear least squares fit to the initial loading and unloading portion of each hysteresis loop from 6 to 25 N (~3–14%) and 140 to 170 N (~82–95%), respectively. Creep strain was defined as the accumulated strain during fatigue and determined from the minimum deflection for a given loading cycle (Fig. 2b).

The modulus or stiffness degradation at a given number of loading cycles was normalized by the initial value measured for the first loading cycle, making a given measure of stiffness degradation equivalent to modulus degradation. Moreover, note that for load control and normalization, the measured LEBT modulus degradation, secant modulus degradation, and creep were equivalent to the strain ratios

$$\text{LEBT}: \frac{E}{E_o} = \frac{\varepsilon_{e,o} + \varepsilon_{p,o}}{\varepsilon_{e,n} + \varepsilon_{p,n}} \quad (3)$$

$$\text{Secant}: \frac{E}{E_o} = \frac{\varepsilon_{e,o}}{\varepsilon_{e,n}} \quad (4)$$

$$\text{Creep}: \frac{\varepsilon_{p,o}}{\varepsilon_{p,n}} \quad (5)$$

where e and p are used by common convention to denote the elastic (recovered) and "plastic" (accumulated) strains, and o and n denote the initial and nth loading cycle, respectively. Note that the accumulated deformation during fatigue is hereafter, and more accurately, termed creep. Eqs. (3)–(5) enabled direct comparison of the measured modulus degradation to the creep strain ratio. Finally, note that each reported strain ratio was equivalent to the corresponding deflection ratio (Fig. 2b), since the dimensions of all specimens were identical.

The total number of linear microcracks, microcrack density (Cr.Dn), and microcrack length (Cr.Ln) were measured for all fatigue specimens and an additional ten unloaded control specimens. Specimens were stained for 16 h in a 0.5 mM calcein (ICN Biomedicals Inc., Aurora, OH) solution under vacuum (≈50 mm Hg) (O'Brien et al., 2003). Each specimen was subsequently dried by serial alcohol dehydration, followed by 90 °C in a vacuum oven overnight, and embedded in poly(methylmethacrylate) (Sample-kwick®, Buehler Ltd., Lake Bluff, IL). Embedded specimens were sectioned longitudinally into 250-μm-thick sections using a low-speed diamond wafer saw, ground to 150 μm and polished to 1 μm final finish. Each section was mounted on a slide and imaged at 100X magnification using an optical microscope (Eclipse ME600L, Nikon Instruments

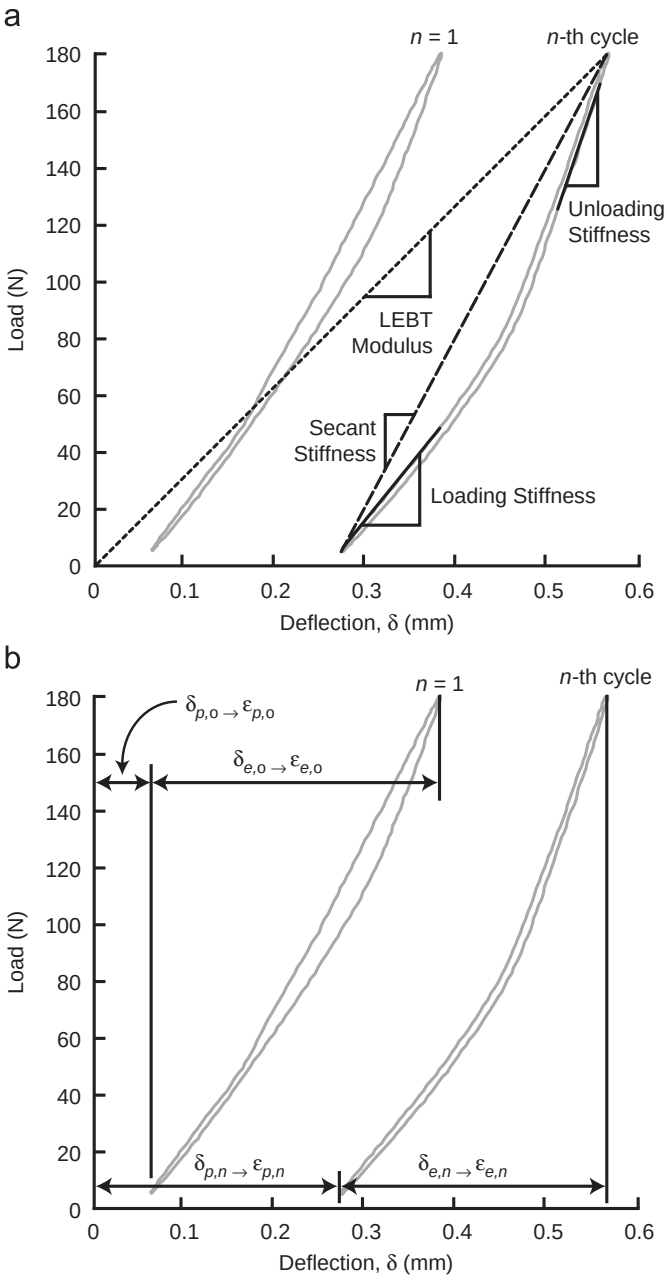

Fig. 2. Hysteresis loops for cyclic four-point bending fatigue of a representative specimen at the initial and final loading cycle showing various mechanical measures of damage in terms of (a) stiffness or modulus, and (b) deflection or strain for elastic, *e*, (recovered) and "plastic", *p*, (accumulated) deformation at the initial, *o*, and *n*th loading cycle. Note that the accumulated deformation during fatigue is hereafter, and more accurately, termed creep. Also, note that in the second experiment conversion of a beam deflection into strain was not necessary since all measures of mechanical degradation were reported by a normalized stiffness or strain ratio (Eqs. (3)–(5)), which was equivalent to the corresponding deflection ratio since the dimensions of all specimens were identical.

Inc., Melville, NY) under green epifluorescence with a fluorescein isothiocyanate (FITC) filter with 460–500 nm excitation and 510–560 nm emission. The number and length of microcracks stained by calcein were measured (O'Brien et al., 2003; Lee et al., 1998), not including microcracks within tissue immediately adjacent to roller supports.

2.3. Statistical methods

Experimental groups were compared using one and two-way analysis of variance (ANOVA) (JMP 5.1, SAS Institute Inc., Cary, NC). Post-hoc comparisons were performed using an unpaired Student's *t*-test or, in the case of microcrack density, a Wilcoxon rank-sum test. The level of significance for all tests was set at 0.05. For experiment 1, the initial LEBT modulus was fit to the applied preload by nonlinear least squares regression using a power law.

3. Results

3.1. Experiment 1: effects of the preload level

The initial specimen modulus defined by LEBT increased nonlinearly with an increased preload level ($p<0.0001$, ANOVA) (Fig. 1). The difference in LEBT modulus between groups with an increasing and decreasing preload level was not statistically significant overall ($p=0.22$, ANOVA) or at any preload level ($p>0.23$, *t*-test), indicating that damage did not accumulate during the course of preloading. Thus, variability for a given preload level was simply due to tissue heterogeneity and the specimens were randomly reassigned to two new groups for fatigue testing. Specimens normalized to 6000 μstrain by an initial modulus measured at a 200 N preload level exhibited a 24% higher initial LEBT modulus (Fig. 1) and were consequently tested in fatigue at a correspondingly higher load level than those normalized using the conventional 100 N preload level. Therefore, specimens that were normalized by measuring the initial specimen modulus at a 200 N preload level experienced a 39% greater relative modulus degradation, or an 8% absolute difference, after 400,000 cycles compared to specimens preloaded at 100 N ($p<0.05$, *t*-test) (Fig. 3). Overall, the modulus degradation of specimens normalized by the two preload levels exhibited a statistically significant difference by group ($p<0.0001$, ANOVA) and interaction with the number of cycles ($p<0.05$, ANOVA).

3.2. Experiment 2: mechanical measures of damage accumulation

Different mechanical measures of damage resulted in widely varying estimates of damage accumulation during fatigue. Changes in each mechanical measure of damage were most apparent in the first 50,000 cycles, continuing less rapidly and nearly linearly thereafter (Figs. 4 and 5). The normalized LEBT modulus decreased by 26% ($p<0.0001$, *t*-test), the normalized secant modulus experienced no degradation ($p=0.51$, *t*-test), and the creep strain ratio decreased by 58% ($p<0.0001$, *t*-test), after

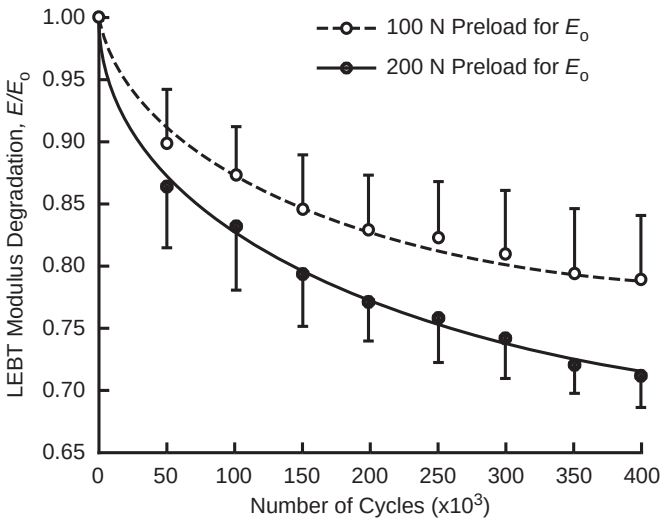

Fig. 3. Modulus degradation, E/E_o, measured using LEBT during load-controlled four-point bending fatigue of specimens normalized to an initial maximum strain of 6000 μstrain using an initial specimen modulus determined at a preload of either 100 or 200 N (Fig. 1). Error bars show one standard deviation.

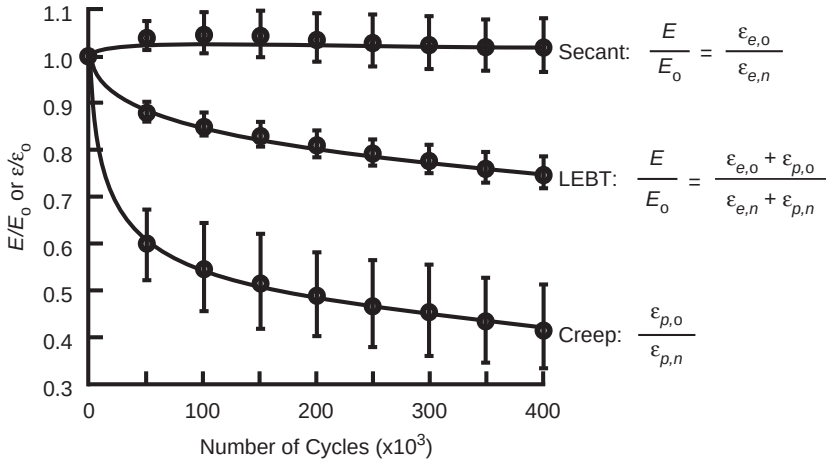

Fig. 4. Mechanical degradation based on measurements of the LEBT modulus (or total strain), secant modulus (or elastic strain), and creep (or accumulated strain) during four-point bending fatigue. Error bars show one standard deviation. Note that the normalized LEBT and secant moduli were equivalent to strain ratios enabling a direct comparison to the creep strain ratio.

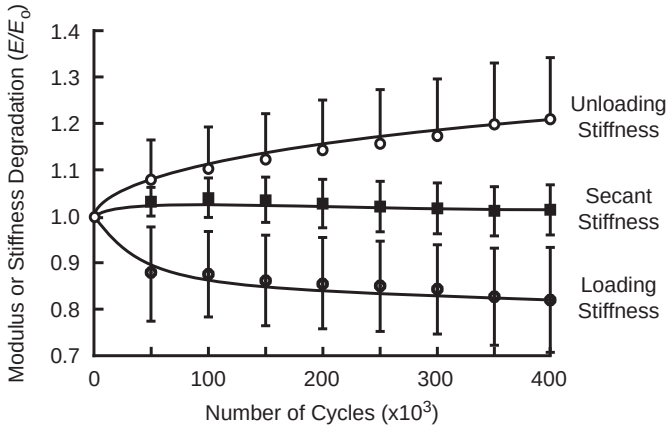

Fig. 5. Mechanical degradation based on measurements of the secant, loading, and unloading stiffness during four-point bending fatigue. Error bars show one standard deviation.

400,000 cycles (Fig. 4). Note that the normalized LEBT and secant moduli were equivalent to strain ratios enabling a direct comparison to the creep strain ratio (Fig. 4). Therefore, the LEBT modulus included effects of both elastic (recovered) and creep (accumulated) strain. The loading and unloading stiffness decreased and increased, respectively, during fatigue ($p<0.0001$, ANOVA) (Fig. 5).

Histology revealed that the microcrack density (Cr.Dn) of specimens loaded to 400,000 cycles at a load normalized to 6000 μstrain was not significantly different from the unloaded control group ($p=0.40$, Wilcoxon rank-sum) (Table 1). The mean crack length (Cr.Ln) increased from 41 ± 22 μm for the unloaded control group to 108 ± 63 μm for the loaded group ($p<0.05$, t-test). Histology further revealed indentation of tissue adjacent to roller supports, with significant sub-surface damage beneath large indentations (Fig. 6). The mean indentation depth per specimen was measured to range between 10 and 63 μm (27 ± 19 μm) and was positively correlated to the creep strain by linear regression ($p=0.06$, $R^2=0.48$).

4. Discussion

Mechanical measures for the accumulation of damage in bovine cortical bone during cyclic four-point bending fatigue were shown to be highly dependent on the methods employed. Therefore, the following recommendations should be considered for standardized four-point bending fatigue tests with cortical bone:

Table 1
The total number of linear microcracks, microcrack density, and microcrack length (mean ± one standard deviation) measured on longitudinal sections for unloaded control specimens compared to specimens loaded to 400,000 cycles with four-point bending fatigue.

Group	Pre-existing (Control)	Loaded	p-Value
Cr.Dn (#/cm^2)	0.26 ± 0.68	0.26 ± 0.45	$p=0.40$[a]
Cr.Ln (μm)	41 ± 22	108 ± 63	$p<0.05$[b]

[a] Wilcoxon rank-sum test.
[b] Unpaired t-test.

4.1. Preloading and normalization

The common protocol using a 100 N preload for 20 cycles significantly underestimated the amount of damage accumulation compared to the use of a higher preload level, which was closer to the level of load employed during the fatigue test after normalizing to the prescribed strain (Fig. 3). Thus, if the LEBT modulus is to be used to normalize tissue heterogeneity, the preload level should be chosen as near as possible to the load level employed during the fatigue test without exceeding the elastic limit for the tissue. The above recommendation minimizes the difference between the level of strain or load employed during preloading and fatigue loading. For example, the 175 N preload level employed in the second experiment corresponded to 5300 ± 300 μstrain compared to 5900 ± 130 μstrain for the initial loading cycles of the fatigue test after normalization to the LEBT modulus.

Alternatively, the secant modulus should be used to determine the initial specimen modulus during preloading instead of the LEBT modulus. The nonlinear dependence of the initial LEBT modulus on the preload level (Fig. 1) caused systematic error in the amount and rate of damage accumulation measured by the LEBT modulus degradation (Fig. 3). However, the secant modulus measured for the same specimens shown in Fig. 1 was independent of the preload level at 17.8 ± 1.8 GPa, which was significantly

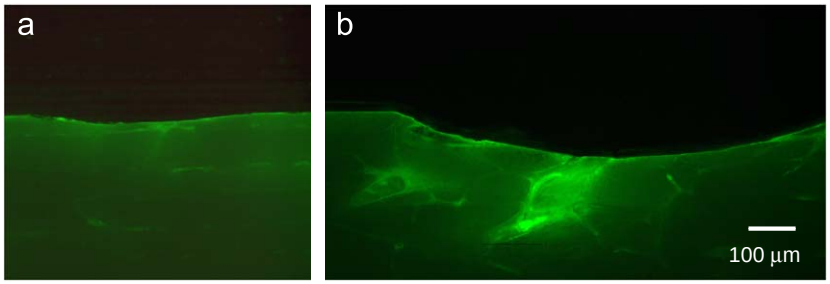

Fig. 6. Optical micrographs using green epifluorescence of calcein-stained longitudinal beam sections showing (a) minimal and (b) significant indentation adjacent to the roller supports. Note the prominence of vasculature within the tissue underlying the larger indentation.

greater than the LEBT modulus measured at any other preload level (Fig. 1).

The nonlinear dependence of the LEBT modulus on the load level (Fig. 1) was not expected and initially thought to be due to strain rate effects (Schaffler et al., 1989), since the strain rate increased with increasing load level. Therefore, an additional five specimens were prepared and loaded from 40 to 300 N in 20 N increments at a constant strain rate by adjusting the frequency at each load level to match the strain rate for a 200 N load at 2 Hz. The LEBT modulus still increased nonlinearly with an increased preload level ($p<0.0001$, ANOVA) suggesting that the dependence was not due to strain rate effects, but indentation of the roller supports into the tissue as discussed further below.

Finally, it is worth reminding that preloading protocol for normalizing fatigue loads to a prescribed strain may account for variability in the initial specimen modulus, but cannot account for differences in the mode of loading (e.g., uniaxial versus bending) and specimen size (e.g., Weibull modulus) between various studies. Moreover, variability in the number of cycles to a prescribed modulus degradation or failure remains high (Boyce et al., 1998; Cotton et al., 2005; Diab et al., 2006; Gibson et al., 1995; Pattin et al., 1996; Pidaparti et al., 2000; Sobelman et al., 2004), with no apparent differences from typical fatigue test data without a normalization procedure.

4.2. Mechanical measures of damage accumulation

Degradation of the LEBT modulus did not alone adequately characterize damage accumulation, but included the combined effect of elastic (recovered) and creep (accumulated) strain (Fig. 4). While the normalized LEBT modulus decreased by 26% and the creep strain ratio decreased by 58% after 400,000 cycles, the normalized secant modulus experienced no degradation and histology revealed no significant differences in microcrack density (Table 1). Therefore, at minimum, both secant modulus and creep should be measured throughout a test to most accurately indicate damage accumulation and account for different damage mechanisms. Fatigue damage due to elastic (recovered) and creep (accumulated) strain is generally thought to correspond to quasi-brittle microcracking and viscoplasticity, respectively (Lemaitre and Desmorat, 2005). Creep observed in cortical bone fatigue has been suggested to be due to microcrack propagation and/or diffuse damage formation (Winwood et al., 2006a,b), which was supported by an increase in the mean crack length measured in this study (Table 1).

The secant modulus did not change during the course of fatigue testing (Fig. 4), which suggested that damage accumulation due to quasi-brittle microcracking was insignificant, as was confirmed through histological analysis. This was not expected for a test normalized to 6000 μstrain after 400,000 cycles (Boyce et al., 1998; Diab et al., 2006; Diab and Vashishth, 2005; Gibson et al., 1995; Sobelman et al., 2004), but a couple of possible explanations exist. First, as mentioned above, the initial LEBT modulus used to normalize fatigue loads to 6000 μstrain was significantly lower than the initial secant modulus. If the specimens in the second experiment had been normalized using the initial secant modulus, the applied fatigue loads would have been at least 20% greater than those employed. Second, the relative effects of elastic and creep strains were only previously investigated in uniaxial fatigue loading of osteonal human cortical bone (Cotton et al., 2003, 2005; Winwood et al., 2006a,b). In this study, fatigue damage of plexiform bovine cortical bone in four-point bending was dominated by viscoplastic creep (Fig. 4).

Differences in the secant, loading, and unloading stiffness degradation (Fig. 5) were due to the presence of asymmetric hysteresis loops (Fig. 2). Hysteresis loops are typically symmetric about the secant, as previously reported for uniaxial tension and compression (Pattin et al., 1996), and therefore exhibit a similar loading and unloading stiffness. However, all specimens in this study exhibited a distinct change in stiffness approximately midway through the hysteresis loop which became more prominent with an increased number of loading cycles (Fig. 2), leading to the unexpected increase in unloading stiffness during fatigue (Fig. 5). If not for this behavior, changes in the unloading stiffness would be expected due to purely elastic recovery, even following prior inelastic deformation, providing a potentially insightful measure of fatigue damage.

The only other group to report hysteresis loops for four-bending fatigue of cortical bone observed the same asymmetric behavior (Gibson et al., 1995; Griffin et al., 1999). The asymmetry was attributed to the formation of "wear grooves" at fixed load supports and was reported to be minimized by using roller supports (Griffin et al., 1997). However, the asymmetry was prominent in this study despite the use of roller supports. A decline in the hysteresis, or energy dissipated per cycle, was observed to occur within the first 50,000 cycles, followed by constant hysteresis thereafter. This behavior suggested the formation of indentations (Fig. 6), rather than "wear grooves." Moreover, the mean indentation depth per specimen was calculated to account for 8 to 48% ($22\pm24\%$) of the creep strain. The largest indentations exhibited significant sub-surface damage, coinciding with prominent vasculature within the tissue adjacent to the roller supports (Fig. 6). In contrast, fully dense synthetic composites with an elastic modulus similar to cortical bone exhibited typical symmetric hysteresis loops during four-point bending fatigue using similar-sized specimens and the same loading fixture (Kane et al., 2008). Finally, since large creep strains were measured during fatigue (Fig. 4) even after accounting for roller support indentations, viscoplastic deformation may have also contributed to the asymmetric hysteresis by producing a curved beam with an altered neutral axis.

In summary, the presence of indentations at roller supports resulted in inflated measures of the LEBT modulus degradation

and creep. Therefore, considering all the above factors, investigations of fatigue microdamage in cortical bone should avoid the use of four-point bending unless no other option is possible. Other well-known limitations in the use of four-point bending tests include specimen size dependency and stressed volume effects.

5. Conclusions

Mechanical measures for the accumulation of damage in bovine cortical bone during four-point bending fatigue were shown to be highly dependent on the methods employed. Therefore, the following recommendations should be considered for standardized four-point bending fatigue of cortical bone:

(1) The initial specimen modulus should not be measured from beam deflections using linear elastic beam theory (LEBT). The initial LEBT modulus was shown to be nonlinearly dependent on the preload level, which subsequently caused systematic error in the amount and rate of damage accumulation measured by the LEBT modulus degradation. The secant modulus was free of this error and is therefore recommended.
(2) Both the secant modulus and creep, at minimum, should be measured throughout fatigue loading to most accurately indicate damage accumulation and account for different damage mechanisms. The LEBT modulus did not alone adequately characterize damage accumulation, but included a combined effect of both elastic (recovered) and creep (accumulated) strain.
(3) Investigations of fatigue microdamage in cortical bone should avoid the use of four-point bending unless no other option is possible. Histology revealed indentation of tissue adjacent to roller supports, with significant sub-surface damage beneath large indentations, accounting for 22% of the creep strain on average. The indentation of roller supports resulted in inflated measures of the LEBT modulus degradation and creep.

Conflict of interest statement

I and my co-authors have no conflicts of interest to disclose regarding our submission entitled, "Systematic error in the measure of microdamage by modulus degradation during four-point bending fatigue of cortical bone," for publication in the *Journal of Biomechanics*.

Acknowledgements

This research was supported by the US Army Medical Research and Materiel Command (W81XWH-06-1-0196) through the Peer Reviewed Medical Research Program (PR054672), and the National Institutes of Health (AR049598).

References

Akkus, O., Knott, D.F., Jepsen, K.J., Davy, D.T., Rimnac, C.M., 2003. Relationship between damage accumulation and mechanical property degradation in cortical bone: microcrack orientation is important. Journal of Biomedical Materials Research 65A (4), 482–488.

Boyce, T.M., Fyhrie, D.P., Clotkowski, M.C., Radin, E.L., Schaffler, M.B., 1998. Damage type and strain mode associations in human compact bone bending fatigue. Journal of Orthopaedic Research 16 (5), 322–329.

Burr, D.B., Turner, C.H., Naick, P., Forwood, M.R., Ambrosius, W., Hasan, M.S., Pidaparti, R., 1998. Does microdamage accumulation affect the mechanical properties of bone? Journal of Biomechanics 31, 337–345.

Caler, W.E., Carter, D.R., 1989. Bone creep-fatigue damage accumulation. Journal of Biomechanics 22, 625–635.

Cotton, J.R., Zioupos, P., Winwood, K., Taylor, M., 2003. Analysis of creep strain during tensile fatigue of cortical bone. Journal of Biomechanics 36, 943–949.

Cotton, J.R., Winwood, K., Zioupos, P., Taylor, M., 2005. Damage rate is a predictor of fatigue life and creep strain rate in tensile fatigue of human cortical bone samples. Journal of Biomechanical Engineering 127 (4), 213–219.

Danova, N.A., Colopy, S.A., Radtke, C.L., Kalscheur, V.L., Markel, M.D., Vanderby, R., McCabe, R.P., Escarcega, A.J., Muir, P., 2003. Degradation of bone structural properties by accumulation and coalescence of microcracks. Bone 33, 197–205.

Diab, T., Vashishth, D., 2005. Effects of damage morphology on cortical bone fragility. Bone 37, 96–102.

Diab, T., Condon, K.W., Burr, D.B., Vashishth, D., 2006. Age-related change in the damage morphology of human cortical bone and its role in bone fragility. Bone 38 (3), 427–431.

Fleck, C., Eifler, D., 2003. Deformation behaviour and damage accumulation of cortical bone specimens from the equine tibia under cyclic loading. Journal of Biomechanics 36, 179–189.

Gibson, V.A., Stover, S.M., Martin, R.B., Gibeling, J.C., Willits, N.H., Gustafson, M.B., Griffin, L.V., 1995. Fatigue behavior of the equine third metacarpus: mechanical property analysis. Journal of Orthopaedic Research 13, 861–868.

Griffin, L.V., Gibeling, J.C., Gibson, V.A., Martin, R.B., Stover, S.M., 1997. Artifactual nonlinearity due to wear grooves and friction in four-point bending experiments of cortical bone. Journal of Biomechanics 30 (2), 185–188.

Griffin, L.V., Gibeling, J.C., Martin, R.B., Gibson, V.A., Stover, S.M., 1999. The effects of testing methods on the flexural fatigue life of human cortical bone. Journal of Biomechanics 32, 105–109.

Gustafson, M.B., Martin, R.B., Gibson, V., Storms, D.H., Stover, S.M., Gibeling, J., Griffin, L., 1996. Calcium buffering is required to maintain bone stiffness in saline solution. Journal of Biomechanics 29 (9), 1191–1194.

Jepsen, K.J., Davy, D.T., 1997. Comparison of damage accumulation measures in human cortical bone. Journal of Biomechanics 30 (9), 891–894.

Joo, W., Jepsen, K.J., Davy, D.T., 2007. The effect of recovery time and test conditions on viscoelastic measures of tensile damage in cortical bone. Journal of Biomechanics 40, 2731–2737.

Kane, R.J., Converse, G.L., Roeder, R.K., 2008. Effects of the reinforcement morphology on the fatigue properties of hydroxyapatite reinforced polymers. Journal of the Mechanical Behavior of Biomedical Materials 1 (3), 261–268.

Lee, T.C., Myers, E.R., Hayes, W.C., 1998. Fluorescence-aided detection of microdamage in compact bone. Journal of Anatomy 193, 179–184.

Lemaitre, J., Desmorat, R., 2005. Engineering Damage Mechanics. Springer, Berlin.

Moreno, L.D., Waldman, S.D., Grynpas, M.D., 2006. Sex differences in long bone fatigue using a rat model. Journal of Orthopaedic Research 24, 1926–1932.

O'Brien, F.J., Taylor, D., Lee, T.C., 2003. Microcrack accumulation at different intervals during fatigue testing of compact bone. Journal of Biomechanics 36, 973–980.

Pattin, C.A., Caler, W.E., Carter, D.R., 1996. Cyclic mechanical property degradation during fatigue loading of cortical bone. Journal of Biomechanics 29, 69–79.

Pidaparti, R.M., Akyuz, U., Naick, P.A., Burr, D.B., 2000. Fatigue data analysis of canine femurs under four-point bending. Biomedical Materials and Engineering 10, 43–50.

Schaffler, M.B., Radin, E.L., Burr, D.B., 1989. Mechanical and morphological effects of strain rate on fatigue of compact bone. Bone 10 (3), 207–214.

Schaffler, M.B., Radin, E.L., Burr, D.B., 1990. Long-term fatigue behavior of compact bone at low strain magnitude and rate. Bone 11 (5), 321–326.

Sobelman, O.S., Gibeling, J.C., Stover, S.M., Hazelwood, S.J., Yeh, O.C., Shelton, D.R., Martin, R.B., 2004. Do microcracks decrease or increase fatigue resistance in cortical bone? Journal of Biomechanics 37, 1295–1303.

Winwood, K., Zioupos, P., Currey, J.D., Cotton, J.R., Taylor, M., 2006a. Strain patterns during tensile, compressive and shear fatigue of human cortical bone and implications for bone biomechanics. Journal of Biomedical Materials Research 79A, 289–297.

Winwood, K., Zioupos, P., Currey, J.D., Cotton, J.R., Taylor, M., 2006b. The importance of the elastic and plastic components of strain in tensile and compressive fatigue of human cortical bone in relation to orthopaedic biomechanics. Journal of Musculoskeletal and Neuronal Interaction 6 (2), 134–141.

Zioupos, P., Wang, X.T., Currey, J.D., 1996. The accumulation of fatigue microdamage in human cortical bone of two different ages in vitro. Clinical Biomechanics 11 (7), 365–375.